

# GPS Signals in a Geosynchronous Transfer Orbit: “Falcon Gold” Data Processing

Thomas D. Powell, Philip D. Martzen, Steven B. Sedlacek, Chia-Chun Chao, *The Aerospace Corporation*,  
Randy Silva, Alison Brown, *NAVSYS Corporation*, Gabriele Belle, *United States Air Force Academy*

## BIOGRAPHY

Dr. Thomas D. Powell is a Senior Member of the Technical Staff in the Satellite Navigation Department at The Aerospace Corporation. He received his B.S. degree in Aeronautical and Astronautical Engineering from Purdue University, his M.S. degree in Aerospace Engineering from the University of Texas at Austin, and his Ph.D. in Aerospace Engineering from UCLA. His current work is focused on orbit determination and space applications of GPS.

Dr. Philip D. Martzen is a Senior Member of the Technical Staff in the Satellite Navigation Department at The Aerospace Corporation. He received his B.S. degree in Physics from UCSB and Ph.D. degree in Experimental Physics from UCSB. Dr. Martzen spent 17 years with Geodynamics Corporation before joining Aerospace in 1997. His current work focuses on orbit determination and early orbit operations.

Dr. Steven Sedlacek is a Senior Engineering Specialist in the Satellite Navigation Department at The Aerospace Corporation. He received his B.S. and M.S. degrees in mathematics from the University of Nevada, Las Vegas, and his Ph.D. degree in Mathematics from Northwestern University. His current work focuses on space surveillance systems.

Dr. C. C. (George) Chao is a Senior Engineering Specialist in the Astrodynamics Department at The Aerospace Corporation. He received his B.S. degree in Mechanical Engineering from National Cheng Kung University in Taiwan, his M.S. and Ae.E degrees in aeronautics from Caltech and his Ph.D. in Engineering (astrodynamics) from UCLA. He is a co-author of a book “Orbital Mechanics” and has over 25 years of experience in orbit dynamics, perturbations and GPS applications.

Dr. Alison Brown is the President of NAVSYS Corporation, which specializes in developing GPS technology. Dr. Brown received her BA and MA in Engineering from Cambridge University, England, a SM in Aeronautics and Astronautics from MIT, and a Ph.D. in Mechanics and Aerospace from UCLA. She has over 15 years experience in GPS receiver design and has eight GPS related patents. She served as the Space Representative for the Institute of Navigation Council in 1993 and has served as the Technical Chairman

and General Chairman for the ION Satellite Division and the ION Annual Meetings. She is a member of the editorial board for GPS World.

Randy Silva is a Software Engineer at NAVSYS Corporation. Mr. Silva received his Bachelor’s Degree from the University of Colorado. He has worked for the last several years developing software for many GPS applications.

Dr. Gabriele Belle is Visiting Scholar in the Department of Astronautics at the United States Air Force Academy where she is responsible for System Integration and Test of the FALCONSAT-1 spacecraft. She also integrated the GPS sensor into the Falcon Gold spacecraft. Previously she was Project Engineer at NAVSYS Corporation. She worked on GPS applications for spacecraft tracking and the Wide Area Augmentation System. She has twelve years of experience in microelectronics and has worked in industry and at the University of Ulm in Germany. She obtained a Ph.D. in Physics from the University of Nijmegen in Holland and the Max Planck Institute for Solid State Physics in Grenoble, France. In 1997 she graduated from the International Space University in Strasbourg, France with a Master of Space Studies degree.

## ABSTRACT

The US Air Force Academy sponsored experiment “Falcon Gold” was flown in November 1997 to measure GPS signals at high orbital altitudes using the NAVSYS TIDGET sensor. This sensor collects and digitizes short intervals of RF energy which can be processed to extract any GPS signals present in the data. In cooperation with NAVSYS and US Air Force Academy personnel, analysts at The Aerospace Corporation obtained and processed the Falcon Gold spacecraft data. The methods and results of the data processing are presented here. The analysis has yielded positive confirmation of GPS signal detection at altitudes approaching geosynchronous orbit, and provides valuable information for future geosynchronous GPS users.

## BACKGROUND

The “Falcon Gold” [1] experiment was designed and constructed by students at the United States Air Force Academy in Colorado Springs. The primary goal of the program was to provide these students with hands-on experi-

ence in the design, procurement, construction and operation of a spacecraft experiment. The secondary goal of “Falcon Gold” was to provide a glimpse of the GPS signal environment at orbital altitudes above the GPS constellation.

The notion of “faster, better, cheaper” spacecraft design and operation played a key role throughout the program [2]. As a result, an emphasis was placed on low-cost, low power, “off-the-shelf” components in the Falcon Gold hardware design. While a significant amount of usable data was obtained in this experiment, the overall goal of the program and the effects of these design choices should be kept in mind when examining the data.

### **Falcon Gold Experiment Design**

The experiment consisted of the Falcon Gold spacecraft and a data collection facility in Colorado Springs, Colorado. The Falcon Gold spacecraft consisted of a sensor, power supply and communications subsystem.

The sensor assembly consisted of a patch antenna and the “TIDGET” sensor, built by NAVSYS Corporation. This sensor is designed for tracking applications using GPS signals. The TIDGET downconverts and samples RF signals and transmits the data to a central processing location where the coder/correlator and navigation solution functions are performed. This design results in a small, lightweight, low-power sensor which is well suited for the Falcon Gold experiment.

In the Falcon Gold design, the experiment package is mounted on the exterior of the Centaur upper stage. RF signals are collected by a 2” patch antenna. The sampled data, along with some spacecraft health and status bits, are transmitted to the ground via a 9600 baud radio modem operating at a carrier frequency of 400.475 MHz. A separate downlink antenna is configured coaxially with the GPS patch antenna such that all data received by the ground station are collected while both the GPS patch antenna and the downlink antenna are pointed towards the Colorado Springs ground station.

The Falcon Gold experiment was powered by 30 Nickel-Metal Hydride (NiMH) batteries, which had an expected orbital lifetime of 15 to 20 days. To maximize the lifetime of these batteries, the Falcon Gold spacecraft would collect a 40 ms “snapshot” of RF data every 5 minutes, entering “sleep mode” between snapshots to conserve battery power.

The onboard timing and control of the Falcon Gold experiment was performed by a microprocessor which activated the subsystems to collect the data, combined the sample data with the health and status bits, time tagged the data and sent it to the Terminal Node Controller (TNC), from which it was downlinked via the modem.

### **Spacecraft Operation and Data Collection**

The Falcon Gold experiment was a secondary payload on the DSCS spacecraft launch. To avoid interference with any aspect of the early orbit operations of the primary mission, the Falcon Gold experiment was programmed to remain inert until after the DSCS/IABS/Centaur spacecraft

had separated from the Centaur upper stage 1500 seconds after launch. The Falcon Gold experiment was activated 8000 seconds after launch, after the DSCS/IABS spacecraft had separated a safe distance from the Centaur.

Upon activation, the Falcon Gold experiment synchronized its internal microprocessor to the “Terminal Node Controller” (TNC) oscillator which had been synchronized to GPS time a number of days before launch. The so called “micro-controller” controlled the data collection and time tagged the GPS data.

The sensor collected 40 ms of sampled data every 5 minutes. The sampled data was divided into 40 one millisecond “segments” for downlink. The experiment required about 20 seconds to power up the sensor, collect the 40 ms data snapshot, transmit the data and return to sleep mode.

### **TIDGET RF Processing**

After passing through a band-pass filter centered on the GPS  $L_1$  frequency (1575.42 MHz), the RF signals are downconverted in several stages to a final intermediate frequency (IF) of 308.888 KHz and sampled at 2 MHz by the TIDGET sensor. The samples are 1-bit only, capturing only the sign of the sampled signal. This sparse sampling technique reduces the power required by the sensor, at the expense of a decrease in signal to noise ratio, although sufficient information remains in the data for correlation and GPS signal detection.

Each data frame consisted of 40 ms of 1-bit samples taken at rate of 2 MHz. The GPS C/A code is modulated onto the  $L_1$  carrier frequency at 1.023 MHz with a chip length of 1023 and a period of 1 ms. Each 40 ms sampling interval produces a data frame consisting of 80,000 1-bit ( $\pm 1$ ) samples. Although the 2 MHz sampling rate of the 1.023 MHz signal is slightly below the Nyquist rate of 2.046 MHz, the following analysis shows that this rate is sufficient for GPS signal detection.

### **FALCON GOLD DATA FEATURES**

Before discussing the signal processing of the Falcon Gold data, it is important to describe some of the features of the data and the factors affecting its collection on orbit and at the ground station.

#### **Data Frame Fragmentation**

The Falcon Gold spacecraft data obtained by Aerospace consisted of a total of 101 data frames, spanning the period from 3 November to 9 November 1997. A total of 28 of these data frames had invalid or incomplete header information due to various error sources in the data collection process. The remaining 73 frames with valid time tags were processed for GPS signal detection.

Of the 73 Falcon Gold data frames with valid time tags, none were complete, uninterrupted 40 millisecond data sequences. All of the frames were “fragmented.” That is, they each had one or more missing segments which were replaced with the “filler” data (alternating 1’s and 0’s.) Figure 1 depicts a typical Falcon Gold data frame, including “good” segments and bad.

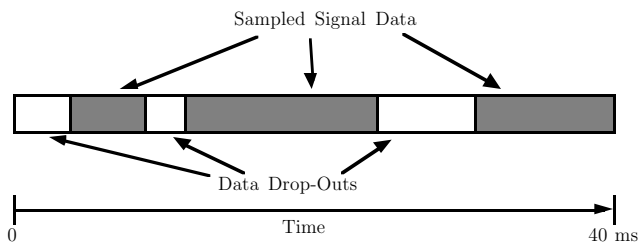


Figure 1: Typical Falcon Gold Data Frame

Fragment length	Number
0 – 5 ms	278
5 – 10 ms	40
10 – 15 ms	14
15 – 20 ms	13
20 – 25 ms	3
25 – 30 ms	4
30 – 35 ms	5

Table 1: Distribution of Falcon Gold Data Fragment Sizes

The approach taken by the Aerospace Corporation was to extract only the good segments from each frame and discard the filler segments. The result was that each frame was divided into a number of “fragments” of varying length containing only valid spacecraft data. The 73 valid data frames were separated into 357 data fragments. Table 1 shows the distribution of the length of the Falcon Gold data fragments. The fragments varied in length from 1 ms to approximately 35 ms.

### Centaur Ephemeris Uncertainty

The Falcon Gold experiment hardware was mounted to the side of the Centaur upper stage which was used to place the DSCS spacecraft into a 35,200 km by 200 km geosynchronous transfer orbit (GTO). Although the combined DSCS/Centaur vehicle was tracked by AFSCN ground stations prior to separation of the DSCS spacecraft, the Centaur itself was not equipped with a SGLS transponder and so could not be actively tracked after separation. Furthermore, the Centaur vehicle performed a number of separation burns and “blow-down” maneuvers to deplete residual fuel after separation. These operations perturbed the Centaur orbit away from the initial DSCS/Centaur GTO so that the SGLS data for the DSCS/Centaur prior to separation was no longer valid for the Centaur after separation. As a result, an accurate ephemeris was not available for the Centaur at the times of Falcon Gold data collection.

The only remaining source of ephemeris information for the Centaur vehicle was the NORAD two-card element set. The accuracy of NORAD elements is typically on the order of a kilometer. This level of accuracy is insufficient for most precise orbit determination applications, but was sufficient for verifying the geometry of the Falcon Gold satel-

lite with respect to the GPS constellation. The NORAD elements were also used as the *a priori* estimate of the Falcon Gold orbit in the orbit determination analysis described later.

### Centaur Attitude Uncertainty

The empty Centaur upper stage to which the Falcon Gold experiment was mounted was essentially space debris at the time of the data collection. Therefore no attitude control was possible. The vehicle is assumed to have been in a slow tumbling motion of approximately 0.1 degrees/second. Furthermore, the attitude of the vehicle was unknown, which had a direct effect on which data reached the ground station.

### Downlink Geometric Constraints

The reception of Falcon Gold data at the ground station in Colorado Springs was the result of a fortuitous set of simultaneous dynamic conditions which could not be controlled by the experiment operators. To obtain data on the ground, the Centaur first had to be visible above the local horizon at Colorado Springs. Secondly, the Centaur had to be in an attitude which pointed the Falcon Gold downlink antenna at the ground station antenna.

The Falcon Gold data obtained by Aerospace covered the period from 3 to 9 November 1997. Assuming data was collected every five minutes, this period represents over 1700 data collection opportunities. The data which Aerospace obtained for this time interval contained only 101 frames, or about 6% of the total number possible. Obviously, most of the data collected by Falcon Gold did not reach the ground due to the restrictive geometric conditions. Fortunately, due to the concept of operations which maximized experiment lifetime, the conditions were met often enough to obtain a useful quantity of data.

### Time Tag Error

The Falcon Gold experiment employed crystal clocks in two of its components, the Terminal Node Controller (TNC) and the microcontroller. The TNC served as a master timing reference for all of the Falcon Gold components and was activated and synchronized with GPS time a few days before launch. At launch +8000 seconds, the TNC commanded the microcontroller to power up and synchronized the microcontroller clock to the TNC clock. Any drift of the TNC clock which had occurred since it was synchronized prior to launch was then transferred to the microcontroller clock as an initial error. The microcontroller clock was then used to time tag the Falcon Gold data frames, subject to the initial error it received from the TNC clock, and its own subsequent drift.

By the time the Falcon Gold data was collected, the TNC clock had been in operation – accumulating error – for approximately two weeks. Because the clocks used were simple, non-space qualified, crystal based units, the time tags placed on the data frames were expected to have significant offsets from the actual time of data collection. Conversations with Air Force Academy personnel involved with the

operation of the Falcon Gold experiment at its ground station revealed that time offsets of several minutes were observed between the data time tags and the ground station's GPS time reference.

The overall uncertainty on the data time tags was therefore assumed to be on the order of several minutes. This time tag uncertainty played no role in the detection of the GPS signals, but it did have a significant impact on the subsequent Falcon Gold-to-GPS visibility calculations and orbit determination.

### TIDGET DATA PROCESSING

The scientific goal of the Falcon Gold experiment was to detect and characterize the strength of the GPS signals at high orbital altitudes. For each GPS signal detected in the Falcon Gold data, signal strength was computed in terms of 'signal to noise ratio' (SNR), or equivalently, in terms of 'carrier to noise ratio', or  $\frac{C}{N_0}$ . This signal strength is computed directly from the results of the signal correlation process. A brief derivation of the GPS signal detection criterion and signal strength estimate is given in this section.

By assuming gain patterns for both the GPS and Falcon Gold spacecraft, and utilizing the geometry of each signal detection, it is also possible to compute a geometric approximation of signal strength for comparison with that obtained from the correlation processing. A derivation of this geometric technique is also given.

### Correlation Processing Overview

Correlation processing was employed to search for GPS coarse acquisition (C/A) code signals. The C/A code is a sequence of 1023 bits with a period of 1 millisecond which is modulated onto the  $L_1$  carrier frequency of 1575.42 MHz using the binary phase shift keying (BPSK) technique [5].

To detect a GPS C/A code sequence, a duplicate copy of the sequence is generated in the receiver and sampled at the same rate as the incoming signal. This locally generated signal is generated with a Doppler shift to account for relative motion between the receiver and GPS spacecraft, and a time shift to account for the travel time of the signal, which then gives the distance to the GPS satellite. The receiver searches for a combination of Doppler shift (or carrier frequency) and time shift (or code phase) that maximize a correlation function between the received and local signal. A simple scalar inner product of the incoming data sequence and the locally generated sequence is used here for the correlation function.

The TIDGET sensor downconverts the  $L$  band RF signals to an intermediate frequency,  $IF_o$ , of 4,308,888.88 Hz (4.30888 MHz), prior to sampling. The signal is then sampled at a rate of 2 MHz, which gives an observable  $IF_o$  of 308,888.88 Hz (308.888 KHz) in the sampled signal. The sample resolution is 1 bit, which captures only the algebraic sign ( $\pm 1$ ) of the sampled signal. The observed  $IF_o$  frequency at which an actual GPS signal is detected will be subject to an offset due to the Doppler shift caused by the

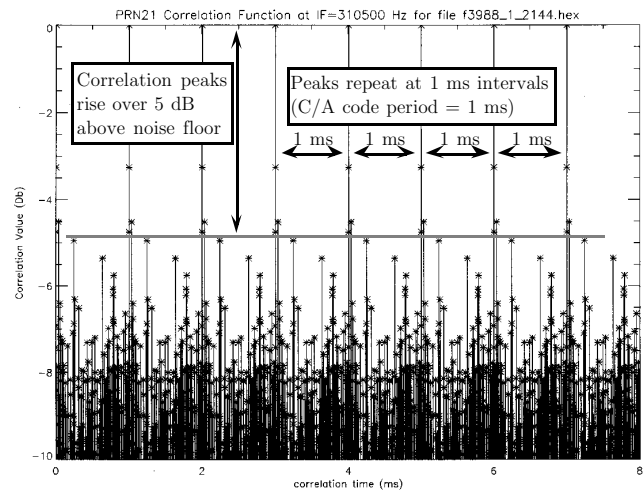


Figure 2: Sample Correlation Plot

relative motion of the Falcon Gold spacecraft with respect to the GPS spacecraft.

A total of 37 C/A pseudorandom number (PRN) codes are available for use by GPS [6], although only 25 GPS satellites were operational in November 1997. Each fragment of Falcon Gold data of sufficient minimum duration (2 ms) was searched over all GPS PRNs and over a Doppler shift range of  $\pm 20$  KHz, in increments of 100 Hz. This maximum Doppler shift corresponds to a maximum relative velocity between GPS and Falcon Gold of approximately  $\pm 4$  km/sec. (Frame 4024, taken near perigee, was searched over  $\pm 50$  KHz to allow a greater relative velocity range of  $\pm 10$  km/sec). GPS signals detected with this "coarse" frequency search were then reprocessed using a "fine" search of 1 Hz increments. Nothing was assumed about the position or attitude of the Falcon Gold spacecraft. This simple "sky search" approach assured that no signal detections would be missed due to false assumptions about the data.

The raw data consisted of sequences of 1-bit samples from the TIDGET sensor of varying length, depending on the length of the data fragment. At the 2 MHz sampling rate, each millisecond of data consisted of 2000 samples, and a complete Falcon Gold data frame of 40 milliseconds contained 80,000 samples.

Figure 2 illustrates a typical GPS signal signature in a time correlation plot. Correlation peaks repeating at 1 ms intervals rise clearly out of the noise floor, as indicated on the plot. This feature indicates GPS signal detection.

### Process Validation with High Altitude Balloon Flight Test Data

The Falcon Gold payload was flown on a high altitude balloon in April 1997 [3] as part of its test program. These tests verified the autonomous operation of the hardware and communications links. Data frames containing GPS signal samples were collected and recorded during the balloon test flights. The sampled data from these balloon tests was ob-

tained and processed at Aerospace as a means of verifying the processing techniques employed for the spacecraft data.

In these tests, the balloon reached an altitude of 105,000 feet and collected a large amount of GPS signal sample data. The sample data collected in these experiments was processed originally by NAVSYS. This analysis showed multiple GPS signals present at all times in the TIDGET sample data, as would be expected for a near-Earth location. Signal strengths from this data were in the 36 – 42 dB range, as predicted.

The particular file of balloon data obtained by Aerospace, when processed by NAVSYS, resulted in the detection of 7 separate GPS PRN codes, the same 7 PRNs detected by NAVSYS. As will be seen, one advantage of the balloon data over the Falcon Gold spacecraft data is that the balloon data frames were all complete, 40 ms long, with valid time tags and header information. Many of the spacecraft data frames were incomplete or corrupted in some way, which complicated the analysis. However, the “clean” balloon data proved crucial in verifying the Aerospace processing techniques.

### GPS Signal Detection and Signal Strength Estimation

Suppose a known BPSK signal,  $S_t$ , is converted to a radio frequency (RF) signal and transmitted through space to a receiving antenna. The received signal is denoted by  $R_t = \alpha S_t + N_t$ , where  $N_t$  is assumed to be a Gaussian white noise process, and  $\alpha$  accounts for the attenuation of the signal by various factors.

The received signal  $R_t$  is assumed to be sampled every  $dt$  seconds as is the locally generated version of  $S_t$ . While the actual transmitted and received signals are analog, the signal detection process deals with sampled data only. Let  $S = \{s_1, s_2, \dots, s_n\}$  denote the sequence of numbers representing the signal  $S_t$  sampled at the rate  $dt$  and  $R = \{r_1, r_2, \dots, r_n\}$  denote the signal  $R_t$  sampled at the same rate. The sampled version of  $R_t$  is also expressed as  $R = \alpha S + N$ , where  $N$  is a discrete time Gaussian white noise sequence.

Let  $T$  be the time interval the signal is being processed over and let  $n$  be the number of samples taken (so  $n = T/dt$ ). The minimum Falcon Gold data segment was 1 millisecond or 2000 bits long, so it is assumed that  $n$  is ‘large’. Let  $(X, Y)$  denote the dot product of  $X$  and  $Y$ , and  $X^2 = (X, X)$  the squared length of  $X$ . Given a random variable  $X$ , let  $E[X]$  denote the expectation of  $X$ . The standard Gaussian random variable with mean zero and variance 1 is denoted by  $Z$ .

To detect a GPS C/A code signal  $S$ , the ‘power’ ratio  $P = \frac{(S, R)^2}{S^2 \sigma^2}$  is computed and if  $P$  exceeds a certain detection threshold value, then the presence of  $S$  is declared. If no signal is present, then  $R = N$  and the random variable  $X = (S, R) = (S, N)$  has mean 0 and variance  $E[X^2] = S^2 \sigma^2$ . Define a second variable  $Y$  as  $Y = \frac{X}{|S| \sigma}$ . Clearly,  $Y$  is distributed as the standard normal random variable  $Z$ .

Therefore,  $P = Y^2$  is distributed as the square of  $Z$ .

An easy computation shows that

$$E[P] = 1 + \frac{\alpha^2 S^2}{\sigma^2}.$$

When no signal is present,  $E[P] = 1$ , as expected from the previous paragraph. The signal to noise ratio ( $SNR$ ) is the ratio of the average signal power divided by the average noise power. In this case, the  $SNR$  is given by:

$$SNR = \frac{\frac{\alpha^2 S^2}{n}}{\frac{E[N^2]}{n}} = \frac{\alpha^2 S^2}{n \sigma^2}$$

Using this expression, and recalling that  $n = T/dt$ , the expression for  $E[P]$  can be rewritten as

$$E[P] = 1 + \frac{SNR}{dt} \cdot T.$$

If no signal is present (meaning  $SNR = 0$ ) then  $E[P] = 1$  as desired.

The signal to noise ratio is related to the carrier to noise ratio by

$$\frac{C}{N_0} = \frac{SNR}{dt}.$$

Substituting this relationship into the equation above gives

$$\frac{C}{N_0} = \frac{P - 1}{T}.$$

This expression shows that the excess of the correlation peak over 1, normalized by the correlation time, gives an estimate for the carrier to noise ratio  $\frac{C}{N_0}$ . Given a detection threshold  $\mathcal{T}$ , GPS signal detection is declared when  $P > \mathcal{T}^2$ , which demands that

$$E[P] = \frac{C}{N_0} \cdot T + 1 > \mathcal{T}^2.$$

This relationship allows trading off  $\frac{C}{N_0}$ ,  $T$ , and detection threshold  $\mathcal{T}$  to see which  $SNR$  levels may be detected from the available data. As expected, the longer the processing time  $T$  is, the weaker  $\frac{C}{N_0}$  may be detected for a fixed detection threshold  $\mathcal{T}$ .

The probability of false alarm, denoted  $P_{fa}$ , is the probability that a sample of the normal random variable  $Z$  mentioned earlier falls outside the range determined by  $\mathcal{T}$ , or

$$P_{fa} = Prob(|Z| \geq \mathcal{T}).$$

For this analysis, in order to avoid false signal detections, a conservative threshold of  $\mathcal{T} = 5$  was used. This gives the corresponding probability of false alarm value of  $P_{fa} = 5.7 \times 10^{-7}$ .

Figure 3 shows a stack histogram distribution of all of the ‘power ratios’ for the ‘coarse’ correlation search ( $\Delta IF =$

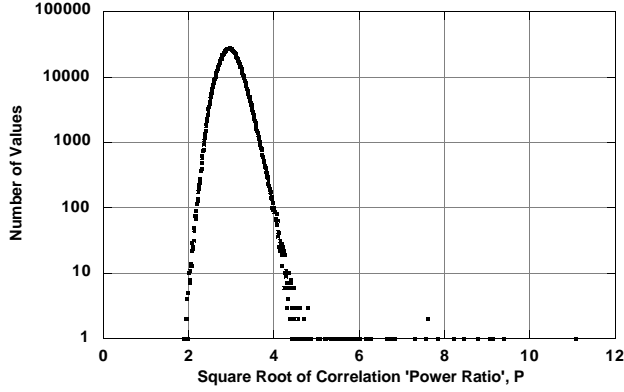


Figure 3: Distribution of Falcon Gold Correlation ‘Power Ratios’

100 KHz) of the Falcon Gold data. The plot is the result of sorting every value of  $\sqrt{P}$  over all Falcon Gold data fragments, GPS PRNs, and Doppler shift values into “bins.” It can be seen from this diagram that the  $\sqrt{P} > T = 5$  signal detection criterion was quite conservative, and that a lower value of  $T$  would have resulted in more GPS signal detections. Given the long list of uncertainty sources and condition of the data, the conservative threshold was used to minimize the probability of a false GPS signal detection.

#### ‘Apparent’ versus ‘Actual’ SNR

The previous derivation assumed that  $\sigma^2$  was known, which is in general not the case. In reality,  $\sigma^2$  needs to be estimated from  $R$ . Assuming that the signal to noise ratio is small for GPS signals, and that the number of samples  $n$  is large, it can be shown that  $\sigma^2$  can be estimated by  $\frac{R^2}{n}$ . Then  $P = \frac{n(S,R)^2}{S^2 R^2}$ . For a BPSK signal,  $S^2 = n$ , so  $P = \frac{(S,R)^2}{R^2}$ . To form the correlation function, take the two functions  $S_I = m(t)\cos(2\pi\omega t)$  and  $S_Q = m(t)\sin(2\pi\omega t)$  and define

$$(S, R)^2 = (S_I, R)^2 + (S_Q, R)^2.$$

If  $R = N$ , then

$$(S, N)^2 = (S_I, N)^2 + (S_Q, N)^2.$$

The random variables  $(S_I, N)$  and  $(S_Q, N)$  are normally distributed with zero mean and variance

$$E[(S_I, N)^2] = E[(S_Q, N)^2] = \frac{n}{2}\sigma^2.$$

They are also approximately independent (since  $E[(S_I, N)(S_Q, N)] \approx 0$ ). Hence  $E[(S, N)^2] \approx n\sigma^2$ . Therefore if  $R = N$ , the random variable  $\frac{(S,R)^2}{n\sigma^2}$  has expected value 1 and is the sum of squares of two independent normal random variables with 0 means and variances  $\frac{1}{2}$ . Therefore  $2P = 2\frac{(S,R)^2}{n\sigma^2}$ , is distributed as the sum of squares of two independent random normal variables so is distributed as a Chi-square random variable

with 2 degrees of freedom. This random variable has a well-known analytic distribution function. Evaluating  $P_{fa}$  with this distribution and  $T = 5$  gives  $P_{fa} = 1.4 \times 10^{-11}$ .

Another complication is the carrier frequency,  $\omega$ , is present which requires a search on frequency and phase. By correlating with  $S_I$  and  $S_Q$ , the phase term may be ignored with a 3 dB loss, which gives

$$E[P] \approx 1 + \frac{1}{2} \cdot \frac{SNR}{dt} \cdot T$$

Finally, the 1 bit sampling has a quantization effect on the data which is equivalent to adjusting the SNR term of the power ratio equation by  $\frac{2}{\pi}$ :

$$E[P] \approx 1 + \frac{1}{\pi} \cdot \frac{SNR}{dt} \cdot T$$

The net effect of the carrier phase non-estimation and the quantization appears to be a reduction of  $SNR$  by 5 to 6 dB.

In light of these factors, one can define an ‘apparent’  $SNR$  and an ‘actual’  $SNR$ , which is the  $SNR$  at the antenna which is defined by antenna gains, power, noise temperature, etc. This actual  $SNR$  should be related to the apparent  $SNR_A$  by a bias. In this case, the difference between the actual and apparent SNR appears to be approximately 5 dB. The uncertainty in the Centaur attitude dynamics could mean that large variations of antenna link margin occurred as the vehicle tumbled, which would preclude computation of accurate relationships between  $SNR$  and  $SNR_A$ . The  $SNR_A$  will provide a lower bound for the actual  $SNR$ .

#### Geometric Computation of $\frac{C}{N_0}$

It is possible to approximate  $\frac{C}{N_0}$  using link considerations such as transmission power, antenna gains, space loss, processing loss, noise temperature, noise bandwidth and the geometry of the encounter.

The largest degree of uncertainty in the Falcon Gold data is associated with the GPS patch antenna gain pattern. Some limited gain pattern data was obtained for the patch antenna from the U.S. Air Force Academy. This data was used to approximate the patch antenna gain pattern, which is illustrated in Figure 6.

A typical gain pattern for a GPS II-R  $L_1$  transmit antenna is shown in Figure 5. This figure is intended to illustrate the basic features of the GPS gain pattern such as the main lobe, first null and sidelobe regions. It is based upon measured gain patterns, although is not representative of all SV gain patterns. The actual GPS gain patterns vary from satellite to satellite and with azimuth (cross section angle) for each individual satellite.

Assuming a constant thermal noise temperature, and the power on  $L_1$  for C/A code is  $P_T = 20.4$  watts, then the following expression can be used to approximate the carrier to noise ratio based purely on geometry:

$$\frac{C}{N_0} = 175 + G_R + G_T(\gamma) - 20\log(\rho)$$

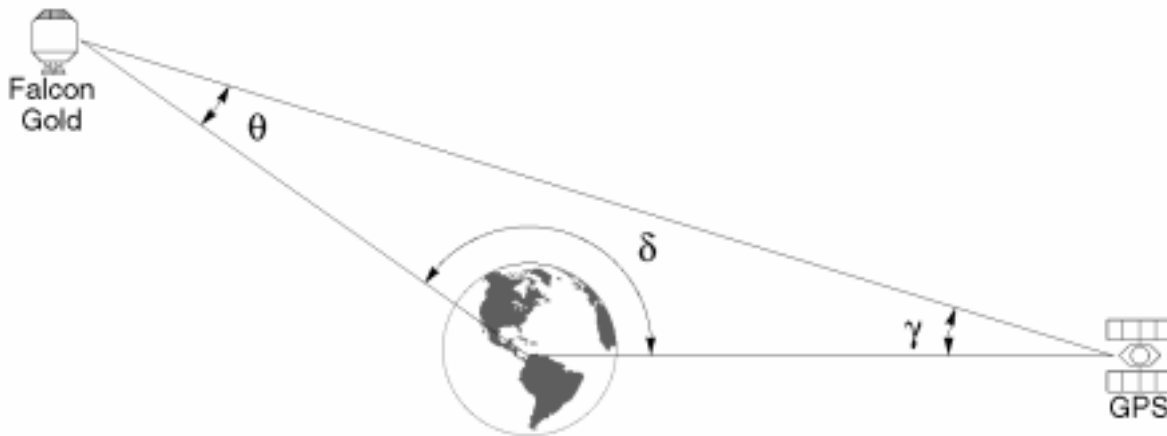


Figure 4: GPS Signal Reception Geometry and Angular Definitions

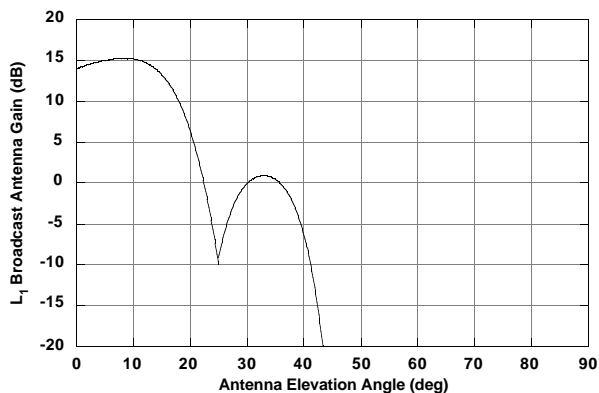


Figure 5: GPS II/II-A gain pattern

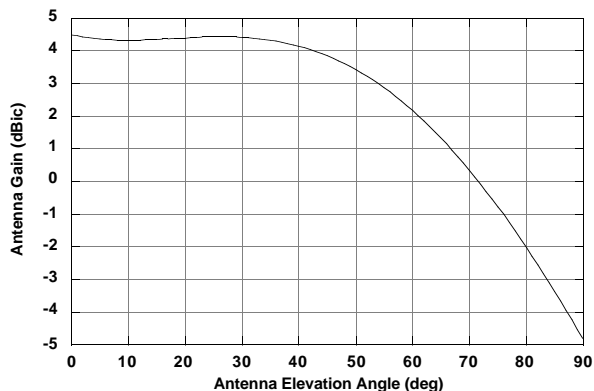


Figure 6: TIDGET patch antenna gain pattern

where  $\frac{C}{N_0}$  is in dBHz,  $G_R$  and  $G_T(\gamma)$  are in dB, and  $\rho$  is the range between the GPS and Falcon Gold spacecraft in meters. Note that the GPS broadcast antenna gain  $G_T(\gamma)$  is a function of the angle  $\gamma$  as described in Figure 4. However, the Falcon Gold patch antenna gain  $G_R$  cannot be directly related to the angle  $\theta$ , due to the attitude uncertainty of the Centaur.

## ORBIT DETERMINATION

The Centaur orbit and Falcon Gold measurement parameters were estimated using a TRACE [8] batch least squares fit of range rate measurements derived from the signal cor-

relation process. The purpose of this exercise was to determine if the observations could be fit to a set of orbit and measurement parameters consistent with the signals detected in the correlation process, and to confirm the relative geometry of the Falcon Gold spacecraft with respect to the ground station and positions of the GPS satellites. The range rate data was also used to resolve the time tag discrepancy noted above.

The Falcon Gold spacecraft orbit had an apogee altitude of approximately 35200 km and a perigee altitude of approximately 200 km. Due to this highly elliptic orbit, atmospheric drag and solar radiation pressure were assumed to be significant perturbation forces and were estimated along with the Falcon Gold orbit parameters.

Covariance analysis indicated a Falcon Gold orbit accuracy on the order of 10 km in position and 3 m/sec in velocity based upon the 2 – 20 m/sec uncertainty on the Doppler range rate measurements and uncertainties in the perturbation force models.

NIMA precise ephemerides [7], which are accurate to approximately 20 cm, were used to compute GPS spacecraft positions. Uncertainty in the RF portion of the Falcon Gold hardware is observable as a range rate bias in the estimation procedure, and so a range rate bias was also estimated.

As discussed above, one constraint on Falcon Gold data collection was the visibility of the vehicle from the ground station in Colorado Springs. Inconsistencies between this geometric constraint and data time tags suggested a time tag offset of approximately 4 minutes. Accordingly, a time tag bias and drift rate were estimated as well.

The Keplerian, J2000 elements for the final Falcon Gold orbit solution, incorporating both the least squares fit of the range rate measurements and the time tag adjustment, are given in Table 4.

Table 3 shows the results of the time tag adjustment procedure for the Falcon Gold data frames where GPS signals were detected. For each frame and fragment, the original unshifted time tag is given along with the shifted time tag and the total number of seconds of the shift. A Falcon Gold clock bias of approximately 4 minutes is seen in the shift

Frame-Fragment Number	Corrected UTC Time Tag (M/D/Y H:M:S)	Time Tag Shift (sec)	Fragment Length (ms)	PRN	Observed Range Rate (m/sec)	Geometric Range Rate (m/sec)	Range Rate Residual (m/sec)
3643-2	11/7/97 16:30:46.1	291.9	26	16	-734.70	-734.74	0.04
3646-1	11/7/97 16:46:54.3	291.7	31	16	-1163.52	-1161.67	-1.85
3649-2	11/7/97 17:03:03.5	291.5	16	16	-1600.62	-1599.27	-1.35
				27	-999.95	-1000.95	1.00
3650-2	11/7/97 17:08:26.6	291.4	17	16	-1747.16	-1746.66	-0.50
3652-1	11/7/97 17:19:12.7	291.3	17	4	-1651.22	-1650.11	-1.11
				16	-2040.17	-2044.10	3.93
3653-2	11/7/97 17:24:35.8	291.2	34	4	-1837.40	-1839.97	2.57
				16	-2186.14	-2188.44	2.30
				19	-2252.91	-2254.14	1.22
				29	-2617.86	-2618.99	1.13
3655-4	11/7/97 17:35:20.9	291.1	17	19	-2430.47	-2432.37	1.90
3656-2	11/7/97 17:40:44.0	291.0	29	4	-2392.49	-2392.96	0.47
				16	-2617.94	-2619.94	2.00
3659-2	11/7/97 17:56:53.1	290.9	31	16	-3033.71	-3037.35	3.64
				19	-2735.94	-2734.58	-1.37
3982-8	11/8/97 22:55:21.3	270.7	8	23	-503.84	-514.04	10.20
4006-1	11/9/97 01:04:31.8	269.2	4	21	-3011.25	-3021.55	10.30
4024-2	11/9/97 02:41:23.9	268.1	8	3	-3100.47	-3102.67	2.20
				15	-5756.76	-5763.25	6.48
				21	-4057.18	-4061.45	4.27
				22	-7999.04	-8008.12	9.08
				23	105.68	105.42	0.26
				27	5013.55	5015.77	-2.21
31	-798.46	-797.39	-1.07				

Table 2: Orbit Determination Summary

Frame Number	Date	Original Time Tag (H:M:S)	Shifted Time Tag (H:M:S)	$\Delta$ sec
3643-2	11/7/1997	16:35:38.000	16:30:46.147	291.853
3646-1	11/7/1997	16:51:46.000	16:46:54.334	291.666
3649-2	11/7/1997	17:07:55.000	17:03:03.521	291.479
3650-2	11/7/1997	17:13:18.000	17:08:26.584	291.416
3652-1	11/7/1997	17:24:04.000	17:19:12.708	291.292
3653-2	11/7/1997	17:29:27.000	17:24:35.771	291.229
3655-4	11/7/1997	17:40:12.000	17:35:20.896	291.104
3656-2	11/7/1997	17:45:35.000	17:40:43.958	291.042
3659-2	11/7/1997	18:01:44.000	17:56:53.145	290.855
3982-8	11/8/1997	22:59:52.000	22:55:21.297	270.703
4006-1	11/9/1997	01:09:01.000	01:04:31.794	269.206
4024-2	11/9/1997	02:45:52.000	02:41:23.917	268.083

Table 3: Falcon Gold Time Tag Adjustment



Semi-Major Axis: 24070 km
Eccentricity: 0.7275
Inclination: 26.296 deg
RAAN: 210.4 deg
Arg. of Perigee: 186.7 deg
Apogee Altitude: 35200 km
Perigee Altitude: 181 km

Table 4: Final Falcon Gold J2000 Orbital Elements

values, as well as a drift of about  $-20$  seconds per day.

A summary of the orbit determination process is presented in Table 2. The fit residuals are consistent with the 2-10 m/sec measurement uncertainty and are seen to decrease with increased sample length and signal strength.

### Geometric Confirmation of GPS Signal Detection

The GPS signals detected in the code correlation process were verified by examining the relative position and velocity of the Centaur with respect to each GPS contact. The NIMA Precise GPS Ephemerides [7] were utilized for this purpose.

For each GPS signal detected in the correlation process, the associated corrected time tag was used to position the Falcon Gold spacecraft at its approximate location when the data was collected. The Falcon Gold ephemeris used for this geometric visibility study was the NORAD elements. This ephemeris is not very accurate, but it was sufficient for the geometry between the GPS and Falcon Gold. The NIMA precise GPS ephemerides were used to position the GPS satellites.

## RESULTS

A total of 25 GPS PRN signals were detected over 12 Falcon Gold data frames. A summary of each Falcon Gold GPS signal detection for the fine (1 Hz) intermediate frequency search resolution and for the  $\mathcal{T} = 5$  detection threshold is presented in Table 5. Each GPS signal detection is described in terms of the length of the data fragment, geometry, and carrier to noise ratio. The angle  $\gamma$  gives the angle of the line of sight to the Falcon Gold spacecraft with respect to the GPS satellite's broadcast antenna boresight. This angle, as depicted in Figure 4, is of particular interest for two of the Falcon Gold data fragments, discussed below.

### GPS Signal Detection Below GPS

The first signal detection of interest occurs in Data Frame 4024, Fragment 2. This data frame was taken at the lowest altitude of any of the frames where GPS signals were detected. This data was taken while the Falcon Gold spacecraft was at an altitude of approximately 1500 kilometers. Note that the distances to the detected GPS satellites are in the range of 3 to 4 Earth radii for this frame, while the distance is in the range of 8 to 10 Earth radii for the other higher altitude detections. PRN 27 was detected while the GPS nadir angle  $\gamma$  was only 11.1 degrees. At GPS altitude, the Earth subtends an angle of approximately 13.5 degrees. Any line of sight from a GPS spacecraft to a receiver on the

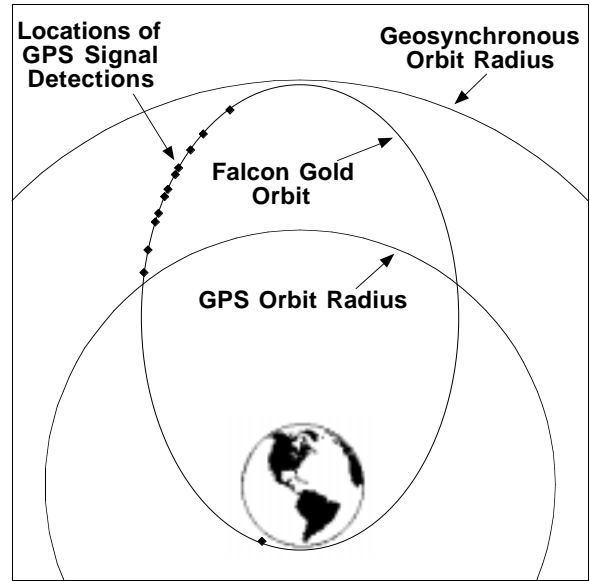


Figure 7: GPS Signal Detection Locations

opposite side of the Earth must form an angle of at least 13.5 degrees with the GPS local nadir. Examining the values of  $\gamma$  in the signal detection detail tables in the appendix, all of the values fall within the interval  $[14 \text{ deg} \leq \gamma \leq 20 \text{ deg}]$  except two. The value of  $\gamma$  and the range to GPS for Frame 4024 – 2 describe a situation where the Falcon Gold spacecraft was below the GPS spacecraft. While the emphasis of the experiment was on high altitude GPS signals, this reception near perigee was somewhat unexpected given the geometric constraints on the data downlink described earlier.

### GPS Sidelobe Signal Detection

The second data segment of particular interest is contained in Frame 3653, Fragment 2. Four GPS PRNs are detected in this fragment. Examining the values of the angle  $\gamma$  for the detected PRNs reveals that PRN 29 was detected at 59.0 degrees, more than 40 degrees further out in the GPS broadcast pattern than the other three PRNs. The geometric range, range rate and signal strength for this PRN are consistent with the other detections shown. By all measures available, this was a valid signal detection. However, examining Figure 5, it is clear that the signal received from PRN 29 did not emanate from the primary lobe of the broadcast antenna, and could only have originated in a *sidelobe* of this SV's antenna pattern.

Because this signal appears to have emanated at such a great angle into the GPS broadcast antenna, it was not possible to compute a GPS antenna gain at this angle using the approximated gain pattern depicted in Figure 5. Therefore, it was not possible to compute a value of  $\frac{C}{N_0}$  based purely on geometry, and no value is listed for this detection.

### Negative Range Rates

A negative value of range rate between a GPS satellite and the Falcon Gold spacecraft indicates that the two were

approaching each other at the time of signal detection. Examining the detailed signal detection tables given in the appendix, the following observation can be made. Range rates for all GPS detections made above the GPS constellation (all but Frame 4024) were uniformly negative, and varied from approximately  $-500$  m/sec to approximately  $-3000$  m/sec. This is the result of two geometric factors, rather than any signal processing effect.

The first is the fact that all of the signal detections were made during the descending half of the Centaur orbit, while it was moving from apogee to perigee. This was due to the downlink requirement of visibility to the Colorado Springs ground station combined with the particular orbital parameters given in Table 4. The argument of perigee was approximately 187 degrees, which placed the ascending node close to the apogee of the orbit. This, combined with the 26 degree orbital inclination and the ground visibility constraint, created a situation where only the descending half of the orbit was visible to Colorado Springs. The ascending half of the orbit was situated below the equator and therefore below the horizon of the ground station.

The second factor contributing to the negative range rates is the direction of the two spacecraft's velocity vectors at the time of signal detection. All of the signal detections above GPS altitude were 'over the limb' detections of GPS spacecraft on the far side of the Earth, as depicted in Figure 4. The line of sight between the GPS spacecraft and the Falcon Gold spacecraft is approximately perpendicular to the GPS spacecraft's velocity vector. This means that the GPS spacecraft velocity contributes little to the relative velocity. Because the Centaur is descending from apogee, its velocity projected onto the line of sight forms the dominant negative term of range rate.

### Other Observations

Figure 7 illustrates the locations of the Falcon Gold spacecraft when GPS signals were detected in relation to geosynchronous altitude and the GPS spacecraft altitude. It shows that all but one of the GPS signal detections occurred well above the GPS constellation altitude. The altitudes of detection ranged from 1500 km above the surface of the Earth to over 33,000 km. The detection range varied from 3 to 10 Earth radii.

Frame number 4024 was sampled near perigee of the GTO. The perigee velocity for the Centaur orbit was approximately 10 km/sec. As mentioned previously, a larger Doppler search range of  $\pm 50$  KHz was used for this frame, and the detections occurred between  $+5000$  and  $-8000$  m/sec.

Carrier to noise ratios ( $\frac{C}{N_0}$ ) computed from the data were consistent with preflight predictions. The computation of the geometric  $\frac{C}{N_0}$  involved rather coarse approximations of both the GPS broadcast antenna pattern (Figure 5) and the Falcon Gold patch antenna pattern (Figure 6). As a result, there are some large errors in the predicted  $\frac{C}{N_0}$  values. However, the predictions show a reasonable level of

agreement and serve as an adequate 'sanity check' on the observed values.

### CONCLUSIONS

The Falcon Gold data processing confirmed that GPS signals can be detected in a GTO using a low cost sensor and a patch antenna. Based on a conservative detection threshold, GPS signals were detected at 12 locations throughout the Centaur GTO. The altitudes of detection ranged from 1500 km above the surface of the Earth to over 33,000 km. The signals were detected under extremely sparse sampling conditions. The ranges to the GPS satellites at which signals were detected ranged from 3 to 10 Earth radii. Carrier to noise ratios ( $\frac{C}{N_0}$ ) computed from the data were consistent with preflight predictions.

When drawing conclusions from the results presented here, it is important to keep in mind that the experiment captured only a few GPS signals over many days of intermittent operation. All of the signal processing was performed post-flight, on the ground. No continuous GPS signal tracking was performed. With these qualifications, however, some useful and potentially promising conclusions can be drawn from the Falcon Gold experiment results.

The results presented here are some of the first examples of GPS signal detection by a spacecraft in a geosynchronous transfer orbit (GTO). The confirmation that GPS signals can be detected throughout a GTO may open the door for future GPS applications for eccentric orbits, especially for launch and early orbit operations. The signals were detected with a low cost, low power sensor and patch antenna which may become a viable alternative to a full featured GPS receiver for certain applications.

The detection of a GPS sidelobe signal presents another technological opportunity. The use of GPS sidelobes for navigation has long been a subject of debate. Use of the GPS broadcast antenna sidelobes for navigation would increase the effective width of the GPS broadcast antenna pattern, providing more signals to high altitude spacecraft. Previous work [9] has shown that increasing the GPS broadcast beam width can significantly improve geosynchronous user navigation accuracy.

While the results presented here are far from conclusive, they do shed some promising light on the use of GPS by high altitude spacecraft in geosynchronous and eccentric transfer orbits. Clearly, further analysis and experimentation are necessary to fully develop this application of GPS.

### REFERENCES

- [1] Belle, G., Matini, A., Brown, A., Goldstein, D., Humble, R., Parker, D., O'Brien, C., "The U.S. Air Force Academy GPS Flight Experiment Using the Navsys TIDGET", Proceedings, ION-GPS 1997, Kansas City, MO, September 16-19, 1997, pp. 717-722.
- [2] Coil, J.A., "Falcon Gold - Orbit Determination Above the GPS Constellation", Proceedings, 11th

Frame-Fragment Number	Fragment Length (ms)	Centaur Altitude (km)	PRN	$\gamma$ (Fig. 4) (deg)	Range (Earth radii)	Observed $\frac{C}{N_0}$ (dBHz)	Geometric $\frac{C}{N_0}$ (dBHz)
3643-2	26.0	31839.9	16	15.7	9.89	34.88	36.07
3646-1	31.0	30688.7	16	14.4	9.74	36.17	37.16
3649-2	16.0	29347.0	16	14.3	9.53	37.92	37.45
			27	14.6	9.48	37.39	37.24
3650-2	17.0	28855.8	16	14.5	9.45	32.79	37.40
3652-1	17.0	27804.8	4	18.7	9.12	34.25	32.98
			16	15.2	9.26	34.28	37.06
3653-2	34.0	27243.8	4	18.6	9.04	30.41	33.15
			16	15.7	9.15	35.90	36.74
			19	14.4	9.19	35.64	37.64
			29	59.0	6.01	30.56	N/A
3655-4	17.0	26049.9	19	15.8	8.95	33.48	36.81
3656-2	29.0	25413.9	4	19.2	8.71	34.81	32.40
			16	17.5	8.79	34.60	35.03
3659-2	31.0	23343.3	16	19.7	8.36	33.90	31.89
			19	18.1	8.43	35.41	34.65
3982-8	8.0	33593.6	23	18.4	10.08	36.23	32.52
4006-1	4.0	21771.4	21	13.8	8.40	39.16	38.84
4024-2	8.0	1550.8	3	16.1	4.46	41.52	39.07
			15	15.9	3.50	42.00	28.38
			21	14.3	4.76	41.19	41.77
			22	14.4	4.75	42.91	41.66
			23	14.6	4.72	41.17	41.40
			27	11.1	3.11	37.11	26.65
			31	17.1	3.73	42.72	30.50

Table 5: GPS Signal Detection Summary

- AIAA/USU Conference on Small Satellites, 15-19 September, 1997.
- [3] O'Brien, C.M., "Falcon Gold - High Altitude Balloon Flight Test of a Fully Integrated Spacecraft", Proceedings, 11th AIAA/USU Conference on Small Satellites, 15-19 September, 1997.
- [4] Brown, A., "The TIDGET - A Low Cost GPS Sensor for Tracking Applications", Proceedings, ION Satellite Division International Meeting, Albuquerque, NM, September 1992.
- [5] Sklar, B., "Digital Communications, Fundamentals and Applications", PTR Prentice Hall, Englewood Cliffs, New Jersey, 1988.
- [6] ICD-GPS-200, Navstar GPS Space Segment/Navigation User Interfaces, Rev. C, 25 September, 1997.
- [7] National Imagery and Mapping Agency's (NIMA) Satellite Geodesy Public Home Page, URL: <http://164.214.2.59/GandG/sathtml/home.html> [10 March 1998].
- [8] Downs, W.D. et. al., "TRACE66, Orbit Determination Program, Volume VII: Usage Guide", Report No. TR-0059(9320)-1, Vol. VII, June, 1971.
- [9] Powell, T.D., Feess, W.A., and Menn M.D., "Evaluation of GPS Architecture for High Altitude Spaceborne Users", Proceedings, Institute of Navigation 54th Annual Meeting, Denver, Colorado, June 1-3, 1998, pp. 157-165.